Coupling Model Interpretation of Thermorheological Complexity in Polybutadienes with Varied Microstructure

Christopher G. Robertson* and Christine M. Rademacher

Bridgestone Americas Center for Research and Technology, 1200 Firestone Parkway, Akron, Ohio 44317-0001

Received August 27, 2004; Revised Manuscript Received October 12, 2004

ABSTRACT: Small-amplitude oscillatory shear rheology was used to investigate relaxation dynamics for two linear polybutadienes with low-vinyl (7% 1,2-addition; PBd-L) and high-vinyl (94% 1,2-addition; PBd-H) microstructures. The M_w values were equal to 38.7 and 80.1 kg/mol for PBd-L and PBd-H, respectively, and both polymers were near-monodisperse ($M_w/M_n < 1.05$). These molecular weights were selected in order to keep the number of entanglements per chain, and hence the plateau length, fairly equivalent for these two polymers. Well-defined terminal flow and segmental relaxation (α-relaxation) loss modulus peaks in the isothermal linear viscoelastic data were used to determine relaxation times, thus the necessity of time−temperature superposition was avoided. These results are interpreted in the context of the Ngai coupling model (CM). We apply the model to both relaxation processes in a unified approach by adopting the CM framework which contends that the primitive relaxation which underlies the cooperative α-relaxation process also directly controls the temperature dependence of the monomeric friction coefficient for the Rouse relaxation, which, in turn, is the primitive process for entangled terminal flow. Thermorheological complexity is a direct consequence of the model, and the viscoelastic data support this prediction for both PBd-L and PBd-H. The common discrepancy between the Vogel temperature evaluated from the temperature dependence of terminal flow and its α-relaxation counterpart is explained and resolved using this coupling model approach.

Introduction

The apparent correspondence of time and temperature dependences of linear viscoelastic response is often used to facilitate accelerated testing and to develop relaxation maps through the formation of master curves using time−temperature superposition. While the failure of such superposition, i.e., thermorheological complexity, for linear amorphous polymers was once considered the exception rather than the rule, its widespread reality is becoming more readily accepted. Plazek and co-workers[1−5] have arguably been the greatest champions for revealing, and providing insight into, failures of time−temperature superposition.

The influence of temperature on relaxation time, τ, can often be different for local segmental motion (α-relaxation process) and terminal flow of polymers, thus thermorheological complexity as a consequence. The well-known Vogel−Fulcher−Tammann−Hesse (VFTH) expression[6−8] can be used to capture these temperature dependences:

$$\tau_\alpha(T) = A_\alpha \exp\left(\frac{B_\alpha}{T - T_{\infty,\alpha}}\right) \quad (1)$$

$$\tau_F(T) = A_F \exp\left(\frac{B_F}{T - T_{\infty,F}}\right) \quad (2)$$

The subscripts α and F denote the α-relaxation and terminal flow processes, respectively. The A, B, and T_∞ are fitting parameters, and T_∞ is often referred to as the Vogel temperature. One outcome of thermorheological complexity is the general observation[9−14] that there exists a crossover of the two functions because the limiting temperature where relaxation times appear to diverge to infinity is lower for terminal flow compared to segmental relaxation, i.e., $T_{\infty,F} < T_{\infty,\alpha}$. This result is a mere product of extrapolating the dissimilar temperature dependences, and the crossover is at odds with physical reality; chain modes cannot be faster than the segmental relaxation which enables them. Of course, this extrapolated crossover occurs within the glassy state where applicability of the segmental VFTH relationship is questionable anyway, even for the case where the glass/liquid is aged to thermodynamic equilibrium.[15,16]

In this contribution, we examine the thermorheological complexity leading to $T_{\infty,F} < T_{\infty,\alpha}$ using new viscoelastic data for two polybutadienes with low-vinyl (7% 1,2-addition; PBd-L) and high-vinyl (94% 1,2-addition; PBd-H) microstructures. The only existing literature which considers in detail the influence of polybutadiene microstructure on rheological behavior encompassing the extensive range from segmental through terminal dynamics is an excellent study by Zorn et al.[17] Compared to this prior work, we use polymers with higher levels of entanglement to introduce more separation between the terminal and segmental processes. Furthermore, we adjust molecular weight to keep this separation nearly equivalent for PBd-L and PBd-H by taking into account the influence of microstructure on the molecular weight between entanglements, M_e. Distinct influences of temperature on local segmental motion and flow of entangled polymers are predicted by the coupling model (CM) of Ngai.[18−21] Using our viscoelastic data on the two polybutadienes, we illustrate that the coupling model not only rationalizes the observation of different temperature dependences but also provides mathematical descriptions of the segmental and terminal flow processes that converge rather than cross at low temperatures.

* Corresponding author: e-mail robertsonchristopher@bfusa.com.

10.1021/ma0482415 CCC: $27.50
Published on Web 12/04/2004

Table 1. Polymer Characteristics

polymer	1,2 [vinyl] (mol %)	*trans*-1,4 (mol %)	*cis*-1,4 (mol %)	M_w (kg/mol)	M_w/M_n	T_g (K)[b]
PBd-L	7	56	37	38.7	1.04	180.8
PBd-H	94	*a*	*a*	80.1	1.03	268.7

[a] *trans*-1,4 + *cis*-1,4 = 6 mol %. [b] DSC midpoint value, 5 K/min heating after cooling into glassy state at 5 K/min.

Experimental Section

The polybutadienes were synthesized by batch anionic polymerization. The reaction vessel was charged with hexane and a solution of 1,3-butadiene in hexane. A polar modifier was added followed by *n*-butyllithium initiation. For PBd-H, the mixture was stirred under N_2 pressure at 13−16 °C for 135 h, reaching 98% conversion of monomer. For PBd-L, the mixture was heated under N_2 pressure to a peak temperature of 86 °C. Both polymer cements were terminated/coagulated in 2-propanol, stabilized with an antioxidant, and dried.

The microstructure of the polybutadienes was analyzed using ^{1}H and ^{13}C NMR (Varian Mercury 300 NMR) with deuterated chloroform as solvent. Gel permeation chromatography (GPC) was performed in THF using a Waters model 150-C with a refractive index detector. GPC measurements were conducted relative to polystyrene standards, and the results were then converted to absolute molecular weight information by applying the universal calibration approach using intrinsic viscosity vs molecular weight control data for the microstructures of interest. Glass transition temperatures were evaluated by differential scanning calorimetry (DSC) (TA Instruments, model DSC 2910) at a heating rate of 5 K/min after cooling into the glassy state at 5 K/min. These characterization results are summarized in Table 1.

A Rheometrics RDAII with a 2000 g cm spring transducer was employed for the isothermal dynamic mechanical shear testing in the segmental/transition region. A parallel plate geometry was used and the plate diameter used was predominately 8 mm although 10 mm diameter plates were used in some cases at the higher temperatures. Sample gaps varied from 2.1 to 2.7 mm. Maximum strains (at outer sample edge) ranged from 0.2 to 0.5%. The small strain oscillatory shear testing involved the use of frequencies from 0.0006 to 100 rad/s. In the plateau/terminal region, a Rheometrics ARES with dual 200 and 2000 g cm force rebalance tranducers was used to make isothermal oscillatory shear measurements. At lower temperatures, parallel plates with 10 mm diameter were used. Testing at higher temperatures employed 25 mm diameter plates. Sample gaps from 1.7 to 2.9 mm were used. Maximum strains varied from 1 to 10%, depending on the measurement temperature. A frequency range from 0.00015 to 100 rad/s was used. Strain sweeps were used to ensure that all oscillatory shear measurements on the two rheometers were well within the linear viscoelastic region.

Results

Segmental Dynamics (α-Relaxation). Viscoelastic results in the segmental/transition region are plotted in Figures 1−4 for the two polybutadienes. The use of a linear scale for the loss modulus in Figures 1 and 3 minimizes any contribution from the lower frequency chain modes of relaxation. The shapes of the segmental loss modulus peaks were similar for each polymer at all of the temperatures explored; hence, approximate superposition in this region appears possible for both PBd-L and PBd-H. In contrast, the corresponding peaks in tan δ, which show up roughly 2 decades lower in frequency, display pronounced thermorheological complexity (see Figures 2 and 4). Because the maxima in tan δ are in a lower frequency window than the segmental G'' peaks, any overlapping contributions from Rouse relaxation are expected to be more prominent. Such a drastic change in the tan δ peak with temperature has been noted before for several polymers.[9−11,22]

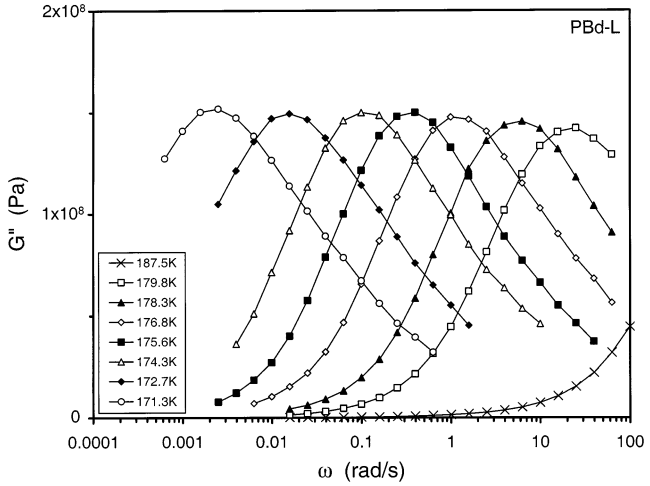

Figure 1. Segmental $G''(\omega)$ for PBd-L at the indicated temperatures.

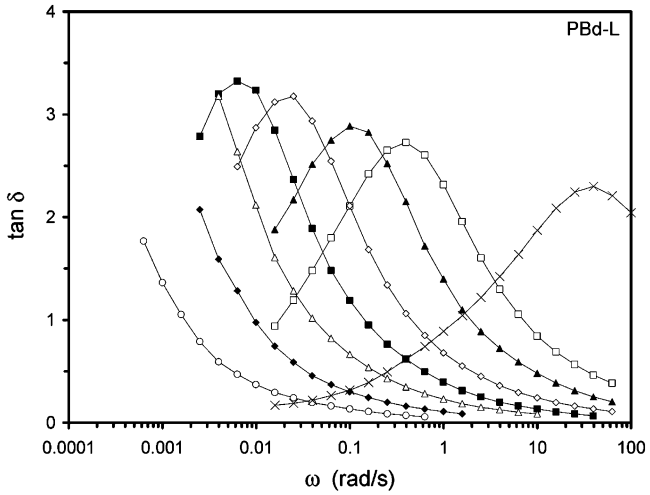

Figure 2. Segmental tan δ for PBd-L. The symbol legend is the same as for Figure 1.

The marked failure of tan δ superposition in this region is anticipated by the coupling model as will be addressed later.

Values of segmental relaxation time were determined from the inverse of the frequency associated with the peak in the loss modulus function, $\tau_\alpha = (\omega_{max})^{-1}$. Assignment of relaxation times in this manner is unbiased and does not rely on superposition of the data. The results are given for the two polybutadienes in Table 2. A fragility plot,[23−25] or cooperativity plot,[26] is given in Figure 5 wherein it is clear that the variation of τ_α with respect to T_g/T is much steeper for PBd-H compared to PBd-L. The slope of the data plotted in this manner at $T = T_g$ yields the fragility, m, which is commonly used to compare the T_g-normalized temperature dependences of segmental relaxation for materials.

The temperature-dependent τ_α data from the dynamic oscillatory shear measurements were combined with dielectric data[27−29] on similar polybutadienes (see Fig-

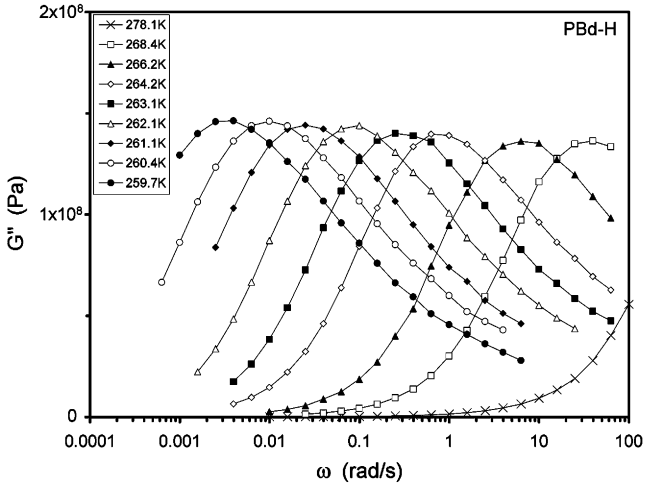

Figure 3. Segmental $G''(\omega)$ for PBd-H at the indicated temperatures.

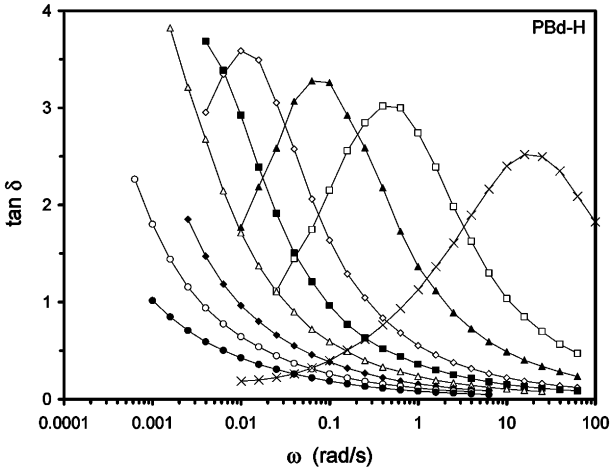

Figure 4. Segmental tan δ for PBd-H. The symbol legend is the same as for Figure 3.

Table 2. Segmental Relaxation Data

PBd-L		PBd-H	
T (K)	τ_α (s)	T (K)	τ_α (s)
171.3	4.27×10^2	259.7	2.99×10^2
172.7	6.54×10^1	260.4	9.71×10^1
174.3	9.17×10^0	261.1	3.64×10^1
175.6	2.60×10^0	262.1	1.05×10^1
176.8	7.44×10^{-1}	263.1	3.62×10^0
178.3	1.69×10^{-1}	264.2	1.17×10^0
179.8	4.55×10^{-2}	266.2	1.46×10^{-1}
		268.4	2.52×10^{-2}

ures 6 and 7). The dielectric results were incorporated in order to extend the segmental data into the temperature range where the terminal relaxation times were acquired. It is well established that the temperature dependences are identical for dielectric and dynamic mechanical α-relaxation times, although the magnitudes of the dielectric τ_α are usually greater.[10,11,30] For polybutadienes, the ratio of dielectric relaxation time to dynamic mechanical relaxation time was previously found to increase with the extent of 1,2 addition in the microstructure.[30] We also noted such an effect; the necessary downward shift of the dielectric data to superimpose with the mechanical τ_α was greater for PBd-H compared to PBd-L (see captions to Figures 6 and 7). The dielectric results of Hofmann et al.[28]and Colmenero et al.[29] for high-vinyl polybutadiene were

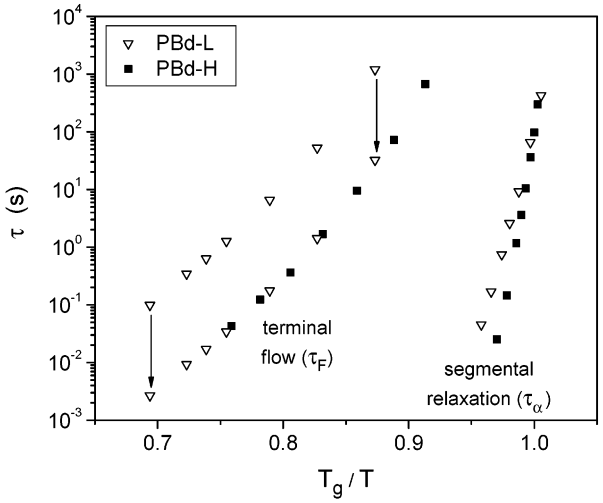

Figure 5. Segmental and terminal relaxation times vs T_g/T for PBd-L and PBd-H. The terminal relaxation times for PBd-L are vertically shifted as shown to allow comparison with the data for PBd-H (see text for discussion). The reference T_g is the temperature at which $\tau_\alpha = 100$ s.

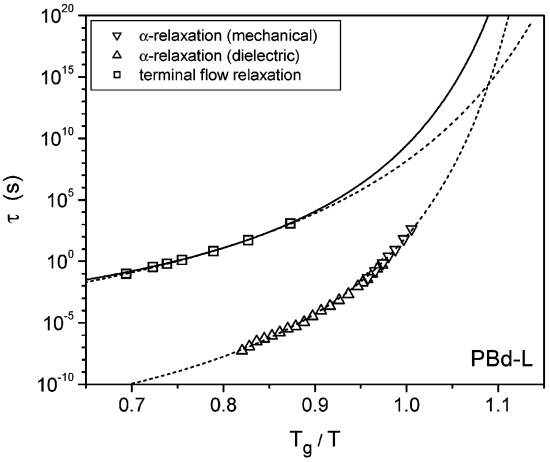

Figure 6. Relaxation times for α-relaxation and terminal flow of PBd-L. The dashed lines are the VFTH fits to the two processes. The solid line is the CM fit to the terminal relaxation data. The reference T_g is the temperature at which $\tau_\alpha = 100$ s. The dielectric data of Arbe et al.[27] are vertically scaled by a factor of $10^{-0.1}$.

used in combination in order to both extend to high temperatures and overlap with the mechanical α-relaxation times of PBd-H. We used the dielectric data of Arbe et al.[27] vs the results of Hofmann and co-workers[28] for low-vinyl polybutadiene because the reported data set is more extensive in temperature range in the former. However, we eschew using the very high temperature ($T > 210$ K) regime where merging of the α-relaxation with the Johari−Goldstein[31] β-process is known to occur for 1,4-polybutadiene.[27,32]

The collective dynamic shear and dielectric data sets for the α-relaxations of PBd-L and PBd-H were fit using the VFTH expression (eq 1), and the parameters are reported in Table 3. Fragility was quantified from the VFTH fitting parameters according to[33,34]

$$m = \left.\frac{\mathrm{d}\log\tau_\alpha}{\mathrm{d}(T_g/T)}\right|_{T=T_g} = \frac{B_\alpha/T_g}{(\ln 10)[1-(T_{\infty,\alpha}/T_g)]^2} \qquad (3)$$

For a reference point, we assigned T_g as the temperature at which $\tau_\alpha = 100$ s; this temperature was evaluated

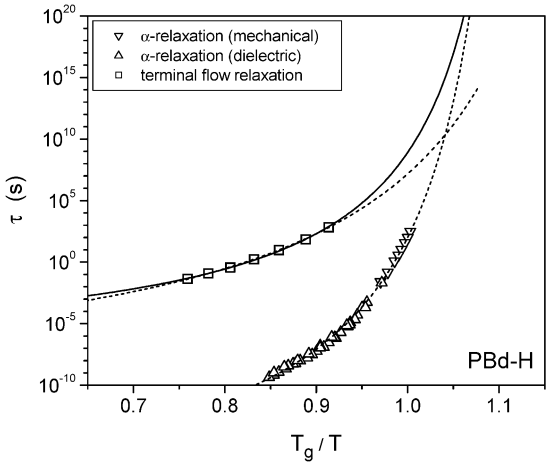

Figure 7. Relaxation times for α-relaxation and terminal flow of PBd-H. The dashed lines are the VFTH fits to the two processes. The solid line is the CM fit to the terminal relaxation data. The reference T_g is the temperature at which $\tau_\alpha = 100$ s. The dielectric data of Hofmann et al.[28] and Colmenero et al.[29] are vertically scaled by factors of $10^{-3.3}$ and $10^{-2.95}$, respectively.

Table 3. Fitting Results for Segmental Relaxation

	VFTH fits					
polymer	A_α (s)	$T_{\infty,\alpha}$ (K)	B_α (K)	T_g[a] (K)	fragility, m	$n_\alpha = 1-\beta$
PBd-L	3.311×10^{-16}	138.1	1374	172.2	88.2	0.53
PBd-H	1.023×10^{-18}	225.6	1601	260.4	149.7	0.60

[a] Temperature at which $\tau_\alpha = 100$ s.

from interpolation of the data using the VFTH fitting results. The derived values of m were 88 and 150 for PBd-L and PBd-H. This stark difference in fragilities for low- and high-vinyl polybutadienes is in agreement with literature results.[17,28,30,35]

The breadths of the segmental relaxations were also contrasted for the low- and high-vinyl polymers using the Kohlrausch−Williams−Watts[36,37] (KWW) equation:

$$G(t) = G_0 \exp[-(t/\tau_K)^\beta] \quad (4)$$

This expression for the time-dependent modulus, $G(t)$, was transformed to the frequency domain to allow fitting of dynamic loss modulus data. In the above, G_0 is the glass modulus, τ_K is the KWW relaxation time, and β is related to the breadth of relaxation response. For $\beta = 1$, the relaxation is exponential (Debye), and the relaxation function breadth increases as β decreases from this value toward its lower limit of zero. The KWW function captures well the shapes of the α-relaxation dispersions for the polybutadienes (Figure 8) with the use of a lower value of β for PBd-H which has a broader, or more nonexponential, response than its low-vinyl counterpart. Breadth of relaxation function and fragility are generally correlated for polymers and other glass-forming liquids.[38] This is true for polybutadienes where it has been noted that fragility and breadth, the latter determined from the quantity $1 - \beta$, both increase with increasing level of 1,2-addition (vinyl content) in the polymer microstructure.[17,35,39] Our results give further confirmation of the connection (Table 3), and the m and β values for PBd-L and PBd-H are in general agreement with the relationship

$$m = 250(\pm 30) - 320\beta \quad (5)$$

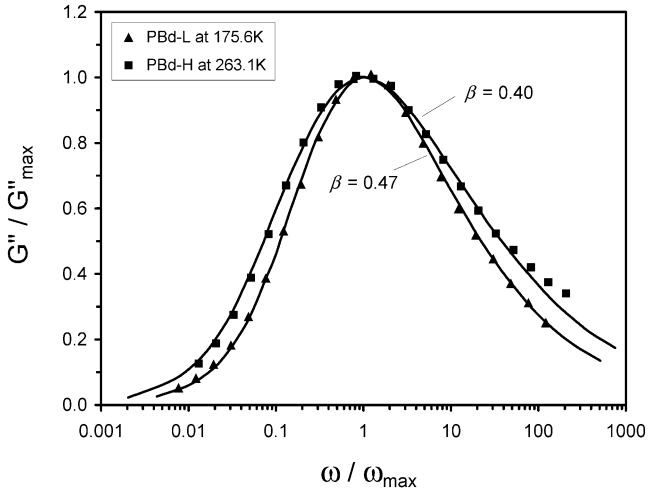

Figure 8. Comparison of segmental dispersion breadths for PBd-L and PBd-H. The lines represent the KWW function fits with the indicated values of β.

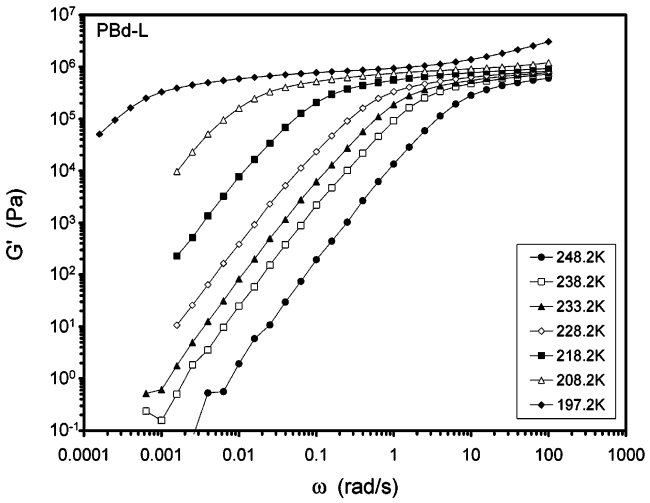

Figure 9. $G'(\omega)$ for PBd-L at the indicated temperatures within the plateau/terminal region.

which was derived from compiled data on many glass formers.[38] Roland and Ngai[39] were the first to note the influence of polybutadiene microstructure on breadth and T_g-normalized temperature dependence associated with segmental dynamics, and they interpreted the results based on enhanced intermolecular cooperativity arising from the steric interactions of the pendant vinyl group.[39,40]

Entanglement Plateau. The molecular weight between entanglements is known to vary with polybutadiene microstructure, with reported values of 1.90 and 3.55 kg/mol for PBd with 7% and 92% vinyl, respectively.[41] For this reason, the molecular weight of the PBd-L investigated in this study was targeted to be about one-half the value of PBd-H. The goal was to maintain the same log(ω) separation between the segmental and terminal dynamics to yield equivalent entanglement plateau lengths for the two polymers. Linear viscoelastic results in the plateau/terminal zones are presented in Figures 9−12. Inspection of the storage modulus data for PBd-L at 197.2 K in Figure 9 with the results for PBd-H at 285.2 K in Figure 11 reveals that the plateau lengths were indeed quite similar.

Table 4. Plateau Moduli and Entanglement Spacings

polymer	M_w (kg/mol)	T (K)	ρ^a (g/cm^3)	G_N (Pa) [eq 6]	G_N (Pa) [eq 7]	M_e^b (kg/mol)	M_w/M_e
PBd-L	38.7	197.2	0.839	8.07×10^5	8.24×10^5	1.69	22.9
PBd-H	80.1	285.2	0.882	6.61×10^5	5.98×10^5	3.32	24.1

[a] Densities are literature values[44] corrected to the indicated temperatures. [b] Calculated using the average of the two G_N values.

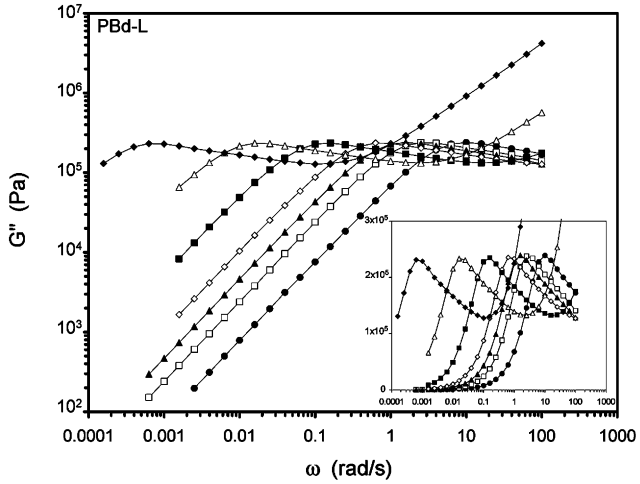

Figure 10. $G''(\omega)$ for PBd-L within the plateau/terminal region. The inset shows the data on a linear y-scale to emphasize the terminal relaxation peaks. The symbol legend is the same as for Figure 9.

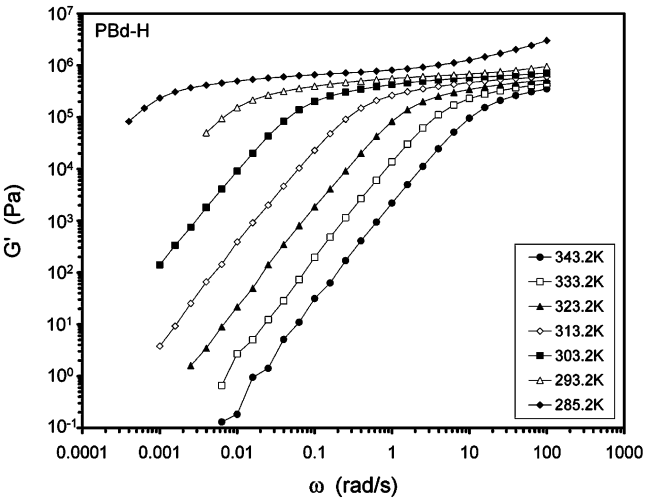

Figure 11. $G'(\omega)$ for PBd-H at the indicated temperatures within the plateau/terminal region.

The plateau modulus, G_N, was calculated from the value of storage modulus where tan δ was at a minimum:[42]

$$G_N = G'|_{\tan \delta_{min}} \tag{6}$$

Also, G_N was evaluated from the maximum loss modulus in the terminal relaxation peak, G''_{max}, using the relationship developed for nearly monodisperse polymer chains by Raju et al.:[43]

$$G_N = 3.56G''_{max} \tag{7}$$

Both of these methods for determining the plateau modulus yielded comparable results (Table 4), and the

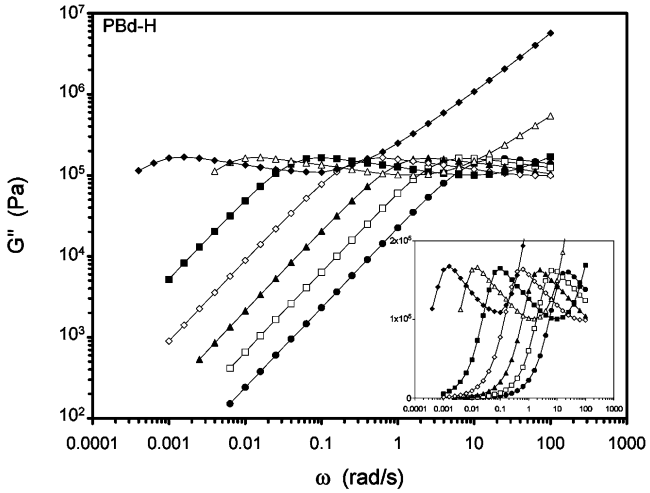

Figure 12. $G''(\omega)$ for PBd-H within the plateau/terminal region. The inset shows the data on a linear y-scale to emphasize the terminal relaxation peaks,. The symbol legend is the same as for Figure 11.

Table 5. Terminal Relaxation Data

PBd-L			PBd-H		
T (K)	τ_F (s)	η_0 (Pa s)	T (K)	τ_F (s)	η_0 (Pa s)
197.2	1.20×10^3		285.2	6.75×10^2	
208.2	5.26×10^1		293.2	7.19×10^1	
218.2	6.58×10^0	7.89×10^6	303.2	9.52×10^0	5.72×10^6
228.2	1.27×10^0	1.57×10^6	313.2	1.69×10^0	9.90×10^5
233.2	6.33×10^{-1}	7.02×10^5	323.2	3.64×10^{-1}	2.35×10^5
238.2	3.44×10^{-1}	3.60×10^5	333.2	1.23×10^{-1}	7.26×10^4
248.2	9.95×10^{-2}	1.18×10^5	343.2	4.31×10^{-2}	2.64×10^4

average value was used for each polymer to determine M_e according to[41]

$$M_e = \frac{\rho RT}{G_N} \tag{8}$$

Values of M_e were calculated to be 1.69 kg/mol for PBd-L and 3.32 kg/mol for PBd-H. These entanglement molecular weights are consistent with the literature values mentioned above. Therefore, the number of entanglements per chain, M_w/M_e, was approximately constant for the two polybutadienes ($M_w/M_e \approx 24$).

Terminal Flow. The time scales for viscous flow of polymers are extended in comparison to the Rouse relaxation process due to entanglements, hence the appearance of the plateau zone. Terminal relaxation is eventually evident in the long time (low frequency) dynamics where a local maximum in loss modulus appears followed by the approach toward the usual terminal scaling of $G' \propto \omega^2$ and $G'' \propto \omega$ as frequency is decreased further (Figures 9−12). The location of the maxima in G'' in this region can be used to designate values of relaxation time associated with terminal flow from $\tau_F = (\omega_{max})^{-1}$. The τ_F results are reported in Table 5. The range of temperatures in which we evaluated τ_F was quite extensive due to the large 6 decade frequency range employed; the observation of terminal G'' peaks at higher or lower temperatures would have required

Table 6. Fitting Results for Terminal Relaxation

	VFTH			CM[a]			
polymer	A_F (s)	$T_{\infty,F}$ (K)	B_F (K)	$t_{c,\alpha}$[b] (s)	$t_{c,F}$[b] (s)	C	n_F[c]
PBd-L	1.507×10^{-7}	124.1	1662	2×10^{-12}	4×10^{-9}	4.6×10^{6}	0.45
PBd-H	5.022×10^{-8}	203.3	1902	2×10^{-12}	4×10^{-9}	2.2×10^{7}	0.45

[a] Other necessary parameters for eq 18 are in Table 3. [b] Constant values. [c] Determined from slopes in Figure 14. A constant value of $n_F \approx 0.42$ could also be used. (see text).

experimentally prohibitive measurements at $\omega > 1 \times 10^2$ rad/s (rheometer limitation) or $\omega < 1 \times 10^{-4}$ rad/s (unreasonable time limitation). Zero shear viscosities were also determined from the viscoelastic data according to

$$\eta_0 = \lim_{\omega \to 0} G''/\omega \tag{9}$$

As shown in Figure 5, the terminal relaxation times are greater for PBd-L at a given T_g/T despite the similar M_w/M_e for the two polymers. The main responsibility for this observation can be assigned to the often unappreciated influence on disentanglement flow from the underlying microstructure-dependent segmental relaxation process. This will be further elaborated later. A downward vertical shift of τ_F data for PBd-L illustrates that the temperature dependences of terminal flow are quite similar for PBd-L and PBd-H (Figure 5). Indeed, it was previously illustrated by Carella et al.[44] and Klopffer et al.[45] that shift factors from time−temperature superposition of dynamic mechanical data in the terminal region for polybutadienes with widely varying microstructures could be approximately reduced onto a common curve when compared at a reference temperature corresponding to a fixed temperature difference above T_g.

Given the literature studies and new data described above, it is quite clear that the local segmental dynamics depend more on the polymer microstructure than do the terminal flow chain dynamics. This gives rise to varying severity of thermorheological complexity depending on the microstructure as detailed by Zorn, McKenna, Willner, and Richter.[17] Even though the temperature dependences of τ_α and τ_F can be different, the two relaxation processes are still intimately connected as will now be illustrated using the coupling model (CM).

Discussion

Independent VFTH fitting of segmental and terminal relaxation times (eqs 1 and 2) allows their temperature dependences to be compared for the two polybutadienes. The consequent VFTH parameters are summarized in Tables 3 and 6, and the fits are shown as dashed lines in Figures 6 and 7. For each polymer, the VFTH fit for terminal flow crosses over its segmental counterpart. The VFTH crossover occurs at $T_g/T = 1.08$ for PBd-L and $T_g/T = 1.04$ for PBd-H. The $T_{\infty,\alpha}$ is 14.6 K greater than $T_{\infty,F}$ for PBd-L, and the difference is 22.3 K for PBd-H. These observations indicate that the difference between temperature dependences of segmental and terminal processes is greater for the high vinyl polymer. Both polybutadienes clearly display thermorheological complexity, although it is more severe for PBd-H.

The coupling model of Ngai is a useful tool to interpret distinct influences of temperature on various relaxation processes in materials. Below, we review the essential features of the model when applied to segmental, Rouse, and terminal dynamics. The model is presented in more detail elsewhere.[18−21] We then apply the CM to the viscoelastic relaxation time data for our polybutadienes to illustrate that, when the interrelated physics of the relaxation processes are included in the analysis, the temperature dependences for τ_α and τ_F properly converge rather than cross in the low-temperature limit.

The primitive process $\tau_{0,\alpha}(T)$ governs the independent local relaxation of the molecular segments and underlies the cooperative α-relaxation. At times greater than a characteristic time $t_{c,\alpha}$, cooperativity causes the primitive motions to become correlated, and the strength of this interaction is represented by the coupling parameter, n_α. The consequence is the following derived expression for the temperature dependence of the observed α-relaxation time:[18−21]

$$\tau_\alpha(T) = (t_{c,\alpha}{}^{-n_\alpha} \tau_{0,\alpha}(T))^{1/(1-n_\alpha)} \tag{10}$$

The value of $t_{c,\alpha}$ is of the order of picoseconds.[46] We use $t_{c,\alpha} = 2 \times 10^{-12}$ s for our calculations herein. The coupling parameter for segmental dynamics is simply $n_\alpha = 1 - \beta$. Therefore, a connection between temperature dependence (fragility) and α-relaxation breadth is predicted by the coupling model, in agreement with data on many small molecule and polymeric glass-forming liquids.[38] Rearrangement of eq 10 produces an equation for the primitive relaxation time in terms of the measured cooperative relaxation time:

$$\tau_{0,\alpha}(T) = t_{c,\alpha}{}^{n_\alpha} [\tau_\alpha(T)]^{1-n_\alpha} \tag{11}$$

Substitution of eq 1 allows the incorporation of $\tau_\alpha(T)$ in terms of VFTH parameters:

$$\tau_{0,\alpha}(T) = t_{c,\alpha}{}^{n_\alpha} \left[A_\alpha \exp\left(\frac{B_\alpha}{T - T_{\infty,\alpha}} \right) \right]^{1-n_\alpha} \tag{12}$$

At frequencies below the segmental relaxation regime, the Rouse model describes well the linear viscoelastic response of unentangled polymers. The Rouse relaxation process is linked to the segmental dynamics via the monomeric friction coefficient, $\xi_0(T)$. The expression for the longest Rouse relaxation time, τ_R, is[41,45]

$$\tau_R(T) = \frac{M^2 a^2 \xi_0(T)}{6\pi^2 M_0{}^2 kT} \tag{13}$$

where a^2 is the mean-square end-to-end length per monomer repeat unit, M is the total polymer molecular weight, and M_0 is the molecular weight of the repeat unit. It is reasonably asserted[19] that the monomeric friction factor (ξ_0) in the Rouse relaxation process is proportional to the noncooperative segmental process represented by $\tau_{0,\alpha}$:

$$\xi_0(T) \propto \tau_{0,\alpha}(T) \tag{14}$$

The temperature dependence of chain coil dimensions

(a^2) and the kT contribution in eq 13 are insignificant compared to the variation of ξ_0 with temperature such that the Rouse relaxation time is approximately connected to $\tau_{0,\alpha}$ through a single proportionality constant, C:

$$\tau_R(T) \approx C\tau_{0,\alpha}(T) \tag{15}$$

From the CM perspective, the Rouse model also applies to entangled polymers at very short times ($t < t_{c,F}$, where $t_{c,F} \approx 4 \times 10^{-9}$ s)[20,47] since intermolecular couplings, by means of entanglements, have not yet exerted influence on chain motion. The Rouse process is considered to be the primitive relaxation ($\tau_{0,F}$) which underlies the terminal flow relaxation of entangled polymers:

$$\tau_{0,F}(T) = \tau_R(T) = C\tau_{0,\alpha}(T) \tag{16}$$

The CM relationship for the cooperative terminal flow process of entangled polymers is

$$\tau_F(T) = (t_{c,F}{}^{-n_F}\tau_{0,F}(T))^{1/(1-n_F)} \tag{17}$$

When applied to the terminal relaxation regime of entangled polymers, modifications to the coupling model[20] were introduced to allow good description of the shape of the terminal dispersion in response to indications otherwise using the original version.[48] These changes do not alter the temperature and molecular weight dependences which are the focus here.

The combination of eqs 12, 16, and 17 produces a direct tie between the segmental and terminal dynamics:

$$\tau_F(T) = C^{1/(1-n_F)} t_{c,F}{}^{-n_F/(1-n_F)}\, t_{c,\alpha}{}^{n_\alpha/(1-n_F)} \left[A_\alpha \exp\left(\frac{B_\alpha}{T - T_{\infty,\alpha}}\right)\right]^{(1-n_\alpha)/(1-n_F)} \tag{18}$$

Application of the coupling model to the zero shear viscosity also leads to the following molecular weight relationship:[19−21]

$$\eta_0 \propto M^{2/(1-n_F)} \tag{19}$$

For consistency with the usual 3.3−3.6 power law exponent observed for the molecular weight dependence of viscosity for entangled linear polymers,[41,49−53] the value of n_F should fall within the narrow range from 0.40 to 0.45.[19,54,55] Accordingly, n_F may be considered a constant. With fixed values $t_{c,\alpha} \approx 2 \times 10^{-12}$ s, $t_{c,F} \approx 4 \times 10^{-9}$ s,[20,47] and $n_F \approx 0.42$, it is apparent that determination of only one unknown, C, is necessary to use eq 18 to fit the terminal flow relaxation times from parameters independently acquired from the breadth and temperature dependence of α-relaxation dynamics. To our knowledge, eq 18 is the first explicit mathematical connection made between segmental dynamics and terminal flow of entangled polymers using the coupling model although the interrelationship between the relaxation processes has always been an embedded feature of the model.

A first test of this unified CM approach to segmental and terminal relaxations is to verify the following proportionality (from eqs 16 and 17) using the experimental results:

$$\tau_F(T) \propto [\tau_{0,\alpha}(T)]^{1/(1-n_F)} \tag{20}$$

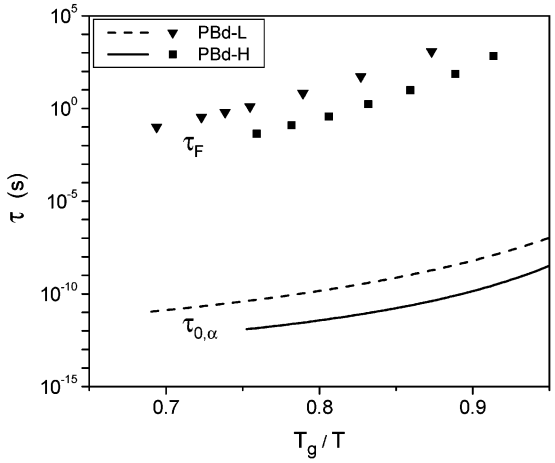

Figure 13. Temperature dependence of τ_F and $\tau_{0,\alpha}$. The latter was determined from segmental dynamics using eq 12.

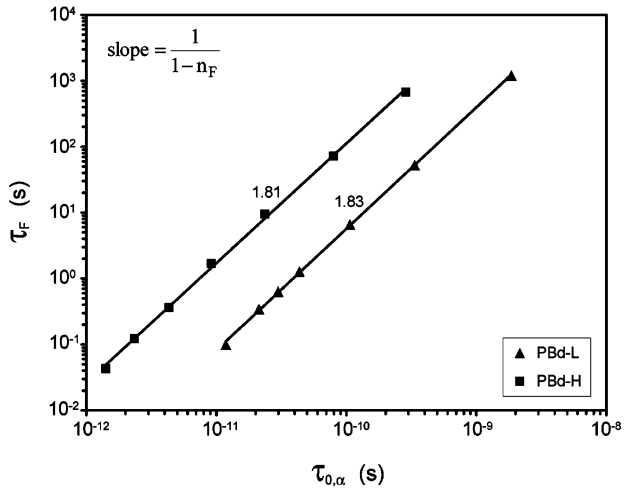

Figure 14. Terminal relaxation times vs primitive α-relaxation time for PBd-L and PBd-H. The values on the plot correspond to the slopes of the given lines.

The $\tau_F(T)$ and $\tau_{0,\alpha}(T)$ are plotted for the polybutadienes in Figure 13. Earlier we pointed out the greater τ_F for PBd-L relative to PBd-H at equivalent T_g/T, notwithstanding the similar M_w/M_e for the two polymers. The source of this difference is now apparent in Figure 13, where $\tau_{0,\alpha}$ is also shown to be greater for the polybutadiene with low vinyl microstructure. A log−log plot of $\tau_F(T)$ vs $\tau_{0,\alpha}(T)$ should provide a straight line with slope $1/(1 - n_F)$ according to eq 20. This is borne out by the results for both polymers in Figure 14. The values of n_F determined from the slopes in Figure 14 were both equal to 0.45 for PBd-L and PBd-H. This n_F yields a realistic molecular weight exponent of 3.6 in eq 19, and this finding lends credence to the approach.

The experimental τ_F data were fit using the coupling model expression given in eq 18 by adjustment of C, the only unknown parameter (see Table 6 and Figures 6 and 7). The values of n_F were predetermined to be equal to 0.45 (corresponding to $\eta_0 \propto M_w{}^{3.6}$) for both polymers using the slope method given above. We also considered the use of $n_F \approx 0.42$ (corresponding to $\eta_0 \propto M_w{}^{3.4}$), which resulted in similar fits, albeit with slightly different

values of C. The extent to which each CM fit effectively represents the data appears to be comparable to the corresponding quality of fit provided by the use of the VFTH equation (eq 2). This is revealed in Figures 6 and 7. Of particular significance is the convergence of the CM temperature dependence of τ_F with the VFTH temperature dependence of τ_α at low temperatures. The prevalent observation that $T_{\infty,F} < T_{\infty,\alpha}$ is evidence that the influences of temperature on segmental and terminal dynamics are often different for polymers. However, this disparity in Vogel temperatures is absent of any physical meaning. Independent VFTH characterization of $\tau_F(T)$ does not make the requisite connection to local segmental motion which is offered by the CM approach.

The coupling model reveals that segmental, Rouse, and terminal relaxation processes are all related to the monomeric friction coefficient, but in different ways:

$$\tau_\alpha(T) \propto [\xi_0(T)]^{1/(1-n_\alpha)}; \quad \tau_R(T) \propto \xi_0(T); \quad \tau_F(T) \propto [\xi_0(T)]^{1/(1-n_F)} \quad (21)$$

From inspection of the relationships above, it is clear that global thermorheological complexity is always expected. The value of n_α can vary from 0.3 to 0.7 depending on the polymer chemistry,[38] while n_F remains constant at ca. 0.42 despite variations in chain microstructure. Even when the coupling parameters are equivalent ($n_\alpha = n_F$) and the consequent temperature dependences are identical for local segmental motion and terminal flow of entangled polymers, thermorheological complexity will still be found in the transition zone due to the different influence of temperature on Rouse dynamics. The τ_R has a weaker connection to the temperature-dependent monomeric friction coefficient compared to both τ_α and τ_F, as shown in eq 21. This leads to the extreme breakdown of time−temperature correspondence for tan δ in the transition region (Figures 2 and 4). This universal failure of superposition is not disconcerting, however, because the three relaxation processes are still fundamentally interconnected as demonstrated in this exercise.

Summary

Temperature can exert different influences on segmental relaxation and terminal flow of polymers. A consequence of this is a lower Vogel temperature for the latter and the associated crossover of the VFTH functions for $\tau_\alpha(T)$ and $\tau_F(T)$. Our viscoelastic data for low-vinyl and high-vinyl polybutadienes are in full agreement with these generalities. The coupling model predicts different temperature dependences for segmental, Rouse, and flow relaxations of entangled polymers yet links all three. Unified application of the CM yields a mathematical description for $\tau_F(T)$, which is dependent upon $\tau_\alpha(T)$ such that the two relaxations merge in the low-temperature limit in a physically sound manner.

Acknowledgment. We are grateful to Bridgestone Americas for permission to publish this research.

References and Notes

(1) Plazek, D. J. *J. Chem. Phys.* **1965**, *69*, 3480.
(2) Plazek, D. J.; Chay, I. C.; Ngai, K. L.; Roland, C. M. *Macromolecules* **1995**, *28*, 6432.
(3) Ngai, K. L.; Plazek, D. J. *Rubber Chem. Technol.* **1995**, *68*, 376.
(4) Plazek, D. J. *J. Rheol.* **1996**, *40*, 987.
(5) Roland, C. M.; Ngai, K. L.; Santangelo, P. G.; Qiu, X. H.; Ediger, M. D.; Plazek, D. J. *Macromolecules* **2001**, *34*, 6159.
(6) Vogel, H. *Phys. Z.* **1921**, *22*, 645.
(7) Fulcher, G. S. *J. Am. Ceram. Soc.* **1925**, *8*, 339.
(8) Tammann, G.; Hesse, W. *Z. Anorg. Allg. Chem.* **1926**, *156*, 245.
(9) Beiner, M.; Reissig, S.; Schroter, K.; Donth, E.-J. *Rheol. Acta* **1997**, *36*, 187.
(10) Ferri, D.; Castellani, L. *Macromolecules* **2001**, *34*, 3973.
(11) Santangelo, P. G.; Roland, C. M. *Macromolecules* **1998**, *31*, 3715.
(12) Plazek, D. J.; O'Rourke, V. M. *J. Polym. Sci., Polym. Phys. Ed.* **1971**, *9*, 209.
(13) Plazek, D. J. *Polym. J.* **1980**, *12*, 43.
(14) Pfandl, W.; Link, G.; Schwarzl, F. R. *Rheol. Acta* **1984**, *23*, 277.
(15) O'Connell, P. A.; McKenna, G. B. *J. Chem. Phys.* **1999**, *110*, 11054.
(16) DiMarzio, E. A. *J. Res. Natl. Inst. Stand. Technol.* **1997**, *102*, 135.
(17) Zorn, R.; McKenna, G. B.; Willner, L.; Richter, D. *Macromolecules* **1995**, *28*, 8552.
(18) Ngai, K. L. *Comments Solid State Phys.* **1979**, *9*, 127.
(19) Ngai, K. L.; Plazek, D. J. *J. Polym. Sci., Polym. Phys. Ed.* **1986**, *24*, 619.
(20) Ngai, K. L.; Plazek, D. J.; Rendell. R. W. *Rheol. Acta* **1997**, *36*, 307.
(21) Ngai, K. L.; Plazek, D. J. *J. Polym. Sci., Polym. Phys. Ed.* **1985**, *23*, 2159.
(22) Cavaille, J. Y.; Corinne, J.; Perez, J.; Monnerie, L.; Johari, G. P. *J. Polym. Sci., Polym. Phys. Ed.* **1987**, *25*, 1235.
(23) Oldekop, V. W. *Glastech. Ber.* **1957**, *30*, 8.
(24) Laughlin, W. T.; Uhlmann, D. R. *J. Phys. Chem.* **1972**, *76*, 2317.
(25) Angell, C. A. *Science* **1995**, *267*, 1924.
(26) Roland, C. M.; Santangelo, P. G.; Plazek, D. J.; Bernatz, K. *J. Chem. Phys.* **1999**, *111*, 9337.
(27) Arbe, A.; Richter, D.; Colmenero, J.; Farago, B. *Phys. Rev. E* **1996**, *54*, 3853.
(28) Hofmann, A.; Alegria, A.; Colmenero, J.; Willner, L.; Buscaglia, E.; Hadjischristidis, N. *Macromolecules* **1996**, *29*, 129.
(29) Colmenero, J.; Alegria, A.; Santangelo, P. G.; Ngai, K. L.; Roland, C. M. *Macromolecules* **1994**, *27*, 407.
(30) Zorn, R.; Mopsik, F. I.; McKenna, G. B.; Willner, L.; Richter, D. *J. Chem. Phys.* **1997**, *107*, 3645.
(31) Johari, G. P.; Goldstein, M. *J. Chem. Phys.* **1970**, *53*, 2372.
(32) Hansen, C.; Richert, R. *Acta Polym.* **1997**, *48*, 484.
(33) Bohmer, R.; Angell, C. A. *Phys. Rev. B* **1993**, *48*, 5857.
(34) Robertson, C. G.; Wang, X. *Macromolecules* **2004**, *37*, 4266.
(35) Robertson, C. G.; Roland, C. M. *Macromolecules* **2000**, *33*, 1262.
(36) Kohlrausch, R. *Pogg. Ann. Phys.* **1854**, *91*, 179.
(37) Williams, G.; Watts, D. C. *Trans. Faraday Soc.* **1970**, *66*, 80.
(38) Bohmer, R.; Ngai, K. L.; Angell, C. A.; Plazek, D. J. *J. Chem. Phys.* **1993**, *99*, 4201.
(39) Roland, C. M.; Ngai, K. L. *Macromolecules* **1991**, *24*, 5315; **1992**, *25*, 1844.
(40) Ngai, K. L.; Roland, C. M. *Macromolecules* **1993**, *26*, 6824.
(41) Ferry, J. D. *Viscoelastic Properties of Polymers*, 3rd ed.; Wiley: New York, 1980.
(42) Wu, S. *Polymer* **1987**, *28*, 1144.
(43) Raju, V. R.; Menezes, E. V.; Marin, G.; Graessley, W. W.; Fetters, L. J. *Macromolecules* **1981**, *14*, 1668.
(44) Carella, J. M.; Graessley, W. W.; Fetters, L. J. *Macromolecules* **1984**, *17*, 2775.
(45) Klopffer, M.-H.; Bokobza, L.; Monnerie, L. *Polymer* **1998**, *39*, 3445.
(46) Roland, C. M.; Ngai, K. L.; Lewis, L. J. *J. Chem. Phys.* **1995**, *103*, 4632.
(47) Butera, R.; Fetters, L. J.; Huang, J. S.; Richter, D.; Pyckhout-Hintzen, W.; Zirkel, A.; Farago, B.; Ewen, B. *Phys. Rev. Lett.* **1991**, *66*, 2088.
(48) Santangelo, P. G.; Ngai, K. L.; Roland, C. M. *Polymer* **1998**, *39*, 681.
(49) Fox, T. G.; Flory, P. J. *J. Phys. Colloid Chem.* **1951**, *55*, 221.
(50) Berry, G. C.; Fox, T. G. *Adv. Polym. Sci.* **1968**, *5*, 261.
(51) Colby, R. H.; Fetters, L. J.; Graessley, W. W. *Macromolecules* **1987**, *20*, 2226.
(52) Rochefort, W. E.; Smith, G. G.; Rachapudy, H.; Raju, V. R. Graessley, W. W. *J. Polym. Sci., Polym. Phys. Ed.* **1979**, *17*, 1197.

(53) Raju, V. R.; Smith, G. G.; Marin, G.; Knox, J. R.; Graessley, W. W. *J. Polym. Sci., Polym. Phys. Ed.* **1979**, *17*, 1183.
(54) Rendell, R. W.; Ngai, K. L.; McKenna, G. B. *Macromolecules* **1987**, *20*, 2250.
(55) McKenna, G. B.; Ngai, K. L.; Plazek, D. J. *Polymer* **1985**, *26*, 1651.

MA0482415